BB

Michigan State University

National Superconducting Cyclotron Laboratory

MOMENTUM DEPENDENCE OF THE NUCLEAR MEAN FIELD FROM PERIPHERAL HEAVY-ION COLLISIONS

R. PAK, O. BJARKI, S.A. HANNUSCHKE, R.A. LACEY, J. LAURET, W.J. LLOPE, A. NADASEN, N.T.B. STONE, A.M. VANDER MOLEN, and G.D. WESTFALL

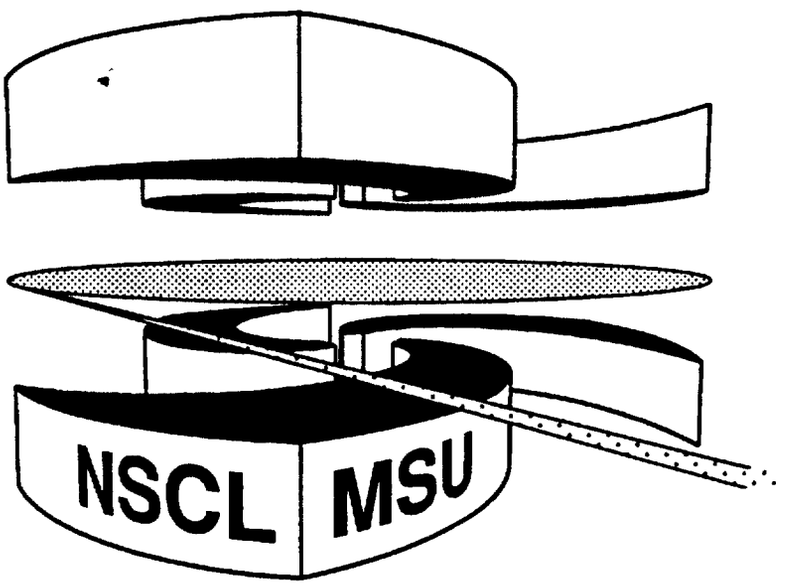

MSUCL-1034 **JULY 1996**

Momentum Dependence of the Nuclear Mean Field from Peripheral Heavy-Ion Collisions

R. Pak,[1] O. Bjarki,[1] S. A. Hannuschke,[1] R. A. Lacey,[2] J. Lauret,[2] W. J. Llope,[3]
A. Nadasen,[4] N. T. B. Stone,[1] A. M. Vander Molen,[1] and G. D. Westfall,[1]

[1] *National Superconducting Cyclotron Laboratory and Department of Physics and Astronomy, Michigan State University, East Lansing, MI 48824-1321, USA*

[2] *Department of Chemistry, State University of New York at Stony Brook, Stony Brook, NY 11794-3400, USA*

[3] *T.W. Bonner Nuclear Laboratory, Rice University, Houston, TX 77251-1892, USA*

[4] *Department of Natural Sciences, University of Michigan, Dearborn, MI 48128-1491, USA*

Abstract

The energy at which collective transverse flow in the reaction plane disappears, the balance energy E_{bal}, is found to increase linearly as a function of impact parameter for ^{40}Ar+^{45}Sc reactions. Comparison of our measured values of $E_{bal}(b)$ with predictions from Quantum Molecular Dynamics (QMD) model calculations agrees better with an approach incorporating momentum dependence in the nuclear mean field.

PACS Numbers: 25.70.Pq, 25.75.Ld

The study of collective flow in heavy-ion collisions can provide information about the nuclear equation of state (EOS), and the parameters involved in the disassembly mechanisms of excited nuclear matter [1, 2, 3, 4]. The mass dependence of the disappearance of directed transverse flow is an example in the intermediate energy regime, from which it was deduced that there is a density dependent reduction of the in-medium nucleon-nucleon cross sections [5, 6]. Collective transverse flow in the reaction plane disappears at an incident energy, termed the balance energy E_{bal} [7], where the attractive scattering dominant at energies around 10 MeV/nucleon balances the repulsive interactions dominant at energies around 400 MeV/nucleon [8, 9, 10]. The disappearance of directed transverse flow has been well established through many experiments [11, 12, 13, 14, 15, 16, 17, 18, 19]. We have recently completed a systematic study of the impact parameter dependence of the disappearance of directed transverse flow, which showed that the balance energy increases approximately linearly as a function of impact parameter in agreement with predictions of Quantum Molecular Dynamics (QMD) model calculations [20, 21]. We have now extended our measurements to higher beam energies for the same projectile-target combination. These data allowed us to extract the balance energies for even larger impact parameters, enabling us to probe the region where the QMD model is sensitive to momentum dependence in the nuclear mean field. Comparison of the balance energies extracted from the measured flow values with predictions from QMD model calculations demonstrates better agreement with a formulation incorporating momentum dependence in the mean field.

The experiments were carried out with the Michigan State University 4π Array [22] at the National Superconducting Cyclotron Laboratory (NSCL) using beams from the K1200

cyclotron. A target of 1.0 mg/cm^2 Sc was bombarded with ^{40}Ar projectiles ranging in energy between 35 and 155 MeV/nucleon in 10 MeV/nucleon steps. Prior to these measurements, the MSU 4π Array was upgraded with the High Rate Array (HRA). The HRA is a close-packed pentagonal configuration of 45 phoswich detectors spanning laboratory polar angles $3° \lesssim \theta \lesssim 18°$. With the HRA, Z resolution up to the charge of the ^{40}Ar projectile and mass resolution for the hydrogen isotopes is obtained. The array has good granularity, minimum dead area, and high data rate capability. Low energy thresholds for the HRA are approximately 13, 15, 32, and 37 MeV/nucleon, for fragments with Z = 1, 3, 12, and 18, respectively.

The main ball of the MSU 4π Array consists of 170 phoswich detectors (arranged in 20 hexagonal and 10 pentagonal subarrays) covering $18° \lesssim \theta_{lab} \lesssim 162°$. The 30 Bragg curve counters (BCCs) installed in front of the hexagonal and pentagonal subarrays were operated in ion chamber mode with a pressure of 125 Torr of C_2F_6 gas. The hexagonal anodes of the five most forward BCCs are segmented, resulting in a total of 55 separate ΔE detectors (the BCCs served as ΔE detectors for charged particles that stopped in the fast plastic scintillator of the main ball). Consequently, the main ball was capable of detecting charged fragments from Z = 1 to Z = 16, with mass resolution for the hydrogen isotopes in the phoswiches. Low energy thresholds were approximately 18, 3.5, and 7 MeV/nucleon for fragments with Z = 1, 3, and 12, respectively. Data were taken with a minimum bias trigger that required at least one hit in the HRA (HRA-1 data), and a more central trigger where at least two hits in the main ball (Ball-2 data) were required. The flow analysis described below was performed with the Ball-2 data as done in Refs. [5, 21].

The impact parameter b of each event is assigned through cuts on centrality variables as calculated through a straightforward geometric prescription [23]. The centrality variable chosen here was $\hat{E}_t$, the reduced transverse kinetic energy of each event, as defined in Ref. [24]. Events with larger values of $\hat{E}_t$ correspond to events with smaller impact parameters. Using methods similar to those detailed elsewhere [25], $\hat{E}_t$ is found to be an appropriate variable to use as a centrality filter for this system over the range of beam energies studied, and it does not autocorrelate with the flow observables. If the measured cross section was equivalent to the geometric cross section, then the maximum impact parameter b_{max} to trigger an event would be the sum of the projectile and target radii $R_{proj} + R_{targ}$. However, $b_{max} < (R_{proj} + R_{targ})$ due to hardware trigger bias and detector acceptance. Comparison of events from the Ball-2 trigger to those from the less selective HRA-1 trigger imply that $b_{max} = 0.88 \pm 0.04(R_{proj} + R_{targ})$. Details of this correction method are provided elsewhere [21]. The impact parameter bins in this flow analysis and the corresponding reduced impact parameters $\hat{b} = (b/b_{max})$ in the simple geometric picture are summarized in Table 1. Also listed in this table are the effective values of the reduced impact parameter corrected for bias due to the hardware trigger condition.

The reaction plane of each event is calculated using the method of azimuthal correlations [26], which is a reliable method to determine the reaction plane in cases where transverse collective motion can become weak (*e.g.* beam energies near the balance energy). First a particle of interest (POI) is chosen from the event. Autocorrelation is suppressed by omitting this POI in the calculation of the reaction plane [27]. The momenta of the remaining particles are projected into a plane perpendicular to the beam axis (taken as the origin in this plane).

A line passing through the origin is then simultaneously fit to the transverse momentum coordinates of these fragments such that the sum of the perpendicular distances to the line is a minimum. The azimuthal angle of this line becomes the azimuthal angle of the reaction plane. The positive half of the reaction plane is defined by the side on which the total transverse momentum in the reaction plane is greatest. Finally, the POI's transverse momentum in the reaction plane p_x is evaluated by projecting it into this calculated reaction plane. This procedure is repeated for each particle in the event for all events with at least four identified particles.

Fig. 1 shows the mean transverse momentum in the reaction plane $\langle p_x \rangle$ plotted versus the reduced center-of-mass (c.m.) rapidity $(y/y_{proj})_{c.m.}$ for six different reduced impact parameter bins. The data are for fragments with $Z = 2$ from 155 MeV/nucleon ^{40}Ar+^{45}Sc collisions, and the $\hat{b}$ bins (as listed in Table 1) are indicated in each panel. The errors shown in each panel are statistical. The data exhibit the characteristic "S-shape" associated with collective transverse flow in the reaction plane, demonstrating the dynamical momentum transfer on opposite sides of the reaction plane. The offsets from the origin occur because no recoil correction was applied in the reaction plane calculation, which does not affect the final values of the flow observables (balance energies) in this analysis [21]. The data shown in Fig. 1 are fit with a straight line over the midrapidity region -0.5 $\leq$ $(y/y_{proj})_{c.m.}$ $\leq$ 0.25. The slope of this line is defined as the directed transverse flow, which is a measure of the amount of collective momentum transfer in the reaction.

The extracted values of the directed transverse flow plotted as a function of reduced impact parameter are shown in Fig. 2 for the 155 MeV/nucleon ^{40}Ar+^{45}Sc data (solid cir-

cles). Also displayed in this figure are the values of the directed transverse flow for five other bombarding energies. The points at 115 MeV/nucleon represent average values from overlapping data sets. The errors shown are the statistical errors on the slopes of the linear fits (the systematic error associated with the range of the fitting region is +3 MeV/c and -1 MeV/c). That collective transverse flow is maximal at some intermediate impact parameter is reasonable because it must vanish at the extrema, *i.e.* for grazing and perfectly central collisions. This behavior is in qualitative agreement with previous results that range in beam energy from 55 MeV/nucleon [16] to 400 MeV/nucleon [2].

Fig. 3 shows the mean transverse momentum in the reaction plane plotted as a function of the reduced center-of-mass rapidity for six bombarding energies. The data are for fragments with $Z = 2$ from semi-central ^{40}Ar+^{45}Sc collisions (BIN3 as listed in Table 1) at an incident beam energy per nucleon as indicated in each panel. The errors shown in each panel are statistical. The data shown in Fig. 3 are fit with a straight line over the midrapidity region $-0.5 \leq (y/y_{proj})_{c.m.} \leq 0.5$ for beam energies $E < 125$ MeV/nucleon. The fitting range was reduced to $-0.5 \leq (y/y_{proj})_{c.m.} \leq 0.25$ for beam energies $E \geq 125$ MeV/nucleon, resulting in lower values of χ^2 per degree of freedom for these fits. This effect is attributed to our detector acceptance, because less of the projectile component contributes to the flow at these higher beam energies as evidenced by the flatness of the data around $(y/y_{proj})_{c.m.} \approx 1.0$ in Panels (e) and (f) as compared to Panels (a) and (b). The directed transverse flow clearly decreases as the beam energy increases, reappearing again at the higher bombarding energies. This effect has been previously observed [7, 13, 15], and was explained as a balance between the attractive mean field and the repulsive nucleon-nucleon scattering.

The extracted values of the directed transverse flow plotted versus the incident beam energy are shown in Fig. 4 for six reduced impact parameter bins (as listed in Table 1). The points at 115 MeV/nucleon again represent average values from overlapping data sets. The errors shown are the statistical errors on the slopes of the linear fits. The curves are third-order polynomials included only to guide the eye. To extract the balance energy E_{bal}, the data for each $\hat{b}$ bin were fit with a second-order polynomial allowing the fitting range to vary until χ^2 per degree of freedom was a minimum. The second-order fits pass through minima for which the value of the abscissa corresponds to the balance energy at each reduced impact parameter $E_{bal}(b)$. Collective transverse flow is assumed to be symmetric in the vicinity of the balance energy, and our measurements are unable to distinguish the sign (+ or -) of the flow, so that a parabolic function is the lowest order symmetric fit that can be used without *a priori* knowledge of E_{bal}. Listed in Table 2 are the measured values of the balance energies for ^{40}Ar+^{45}Sc reactions extracted from these local parabolic fits for each reduced impact parameter bin shown in Fig. 4. We again verified as reported elsewhere [7, 21] that the analytic form of the fitting function does not significantly affect the value of the extracted balance energy. Triangular fits with two lines of different slope produced values of $E_{bal}(b)$ within error of those reported in Table 2, but a larger number of fit parameters are required.

The horizontal shift in the minima of the curves in Fig. 4 clearly indicates that $E_{bal}(b)$ increases as the impact parameter increases, continuing the trend already shown in Ref. [21]. This result is in qualitative agreement with the work of other groups [13], and was even demonstrated through an entirely different analysis that does not require reaction plane determination using correlation functions [19]. Here we are able to extract more definitively

$E_{bal}(b)$ for larger impact parameters because our measurements include more data points above the balance energy.

The present data set also reaffirms as previously reported [5] that the balance energy does not depend on the particle type. This lack of dependence on the fragment's mass is demonstrated in Fig. 5, which shows the excitation functions of the directed transverse flow for three fragment types at a reduced impact parameter bin of $\hat{b} = 0.39$ for ^{40}Ar+^{45}Sc reactions. The minima of the data for the three fragment types occur at the same value of the incident beam energy indicating a common balance energy. This agreement facilitates comparison of the measured values of $E_{bal}(b)$ to predictions of transport models calculations which involve only nucleons. The dependence of the directed transverse flow on the mass of the emitted particle type shown in Fig. 5 is also consistent with the well known increase in magnitude for heavier fragments [2, 5].

Dynamical transport model calculations can incorporate soft and stiff descriptions of the nuclear EOS as well as momentum dependence in the mean field [28, 29, 30, 31, 32]. Predictions of Quantum Molecular Dynamics (QMD) model [20] calculations are displayed in Fig. 6 for a stiff equation of state with momentum dependence (open circles) and without momentum dependence (open squares) for ^{40}Ca+^{40}Ca reactions. These previously published points [20] were calculated for a fixed impact parameter, and are not corrected for the acceptance effects of our detector array. Also shown in this figure are the measured values of the balance energies for ^{40}Ar+^{45}Sc reactions extracted for six reduced impact parameter bins (solid triangles). These experimental values of $E_{bal}(b)$ are plotted at the upper limit of each $\hat{b}$ bin. The errors shown on the measured values of the balance energies are statistical

(the systematic error is estimated to be +5% and -0%). The balance energy has been shown to exhibit little sensitivity to the acceptance effects of our detector array [7], allowing direct comparison between experimental values and unfiltered theoretical results. We find that $E_{bal}(b)$ increases linearly as a function of the impact parameter in agreement with Refs. [20, 21]. The data suggest better agreement with the QMD model calculations which include momentum dependence in the nuclear mean field, in agreement with the results from studies of nucleus-nucleus collisions at higher bombarding energies [3, 32]. Here we are able to place this additional constraint on the nuclear EOS by measuring the balance energies for peripheral heavy-ion collisions.

In summary, measurements up to an incident beam energy of 155 MeV/nucleon for ^{40}Ar+^{45}Sc collisions allowed us to probe the region where sensitivity to momentum dependence of the nuclear mean field is predicted by the QMD model. Our experimental results indicate that the balance energy increases linearly as a function of impact parameter. Comparison of these measured balance energies with predictions from QMD model calculations demonstrates better agreement with an approach incorporating momentum dependence in the nuclear mean field.

We thank D. Craig, R. McLeod, M. Miller, L. Nieman, D. Sisan, and J. Svoboda for their assistance during data collection and reduction. This work was supported by the National Science Foundation under Grant Nos. PHY-92-14992, PHY-95-28844 (NSCL/MSU) and PHY-92-11611 (SUNY).

References

[1] H. Stöcker and W. Greiner, Phys. Rep. **137**, 277 (1986).

[2] H.H. Gutbrod, A.M. Poskanzer, and H.G. Ritter, Rep. Prog. Phys. **52**, 1267 (1989).

[3] Q. Pan and P. Danielewicz, Phys. Rev. Lett. **70**, 2062, 3523 (1993).

[4] G. Peilert, H. Stöcker, and W. Greiner, Rep. Prog. Phys. **57**, 533 (1994).

[5] G.D. Westfall, W. Bauer, D. Craig, M. Cronqvist, E. Gualtieri, S. Hannuschke, D. Klakow, T. Li, T. Reposeur, A.M. Vander Molen, W.K. Wilson, J.S. Winfield, J. Yee, S.J. Yennello, R.A. Lacey, A. Elmaani, J. Lauret, A. Nadasen, and E. Norbeck, Phys. Rev. Lett. **71**, 1986 (1993).

[6] D. Klakow, G. Welke, and W. Bauer, Phys. Rev. C **48**, 1982 (1993).

[7] C.A. Ogilvie, W. Bauer, D.A. Cebra, J. Clayton, S. Howden, J. Karn, A. Nadasen, A. Vander Molen, G.D. Westfall, W.K. Wilson, and J.S. Winfield, Phys. Rev. C **42**, R10 (1990).

[8] J.J. Molitoris and H. Stöcker, Phys. Lett. **162B**, 47 (1985).

[9] G.F. Bertsch, W.G. Lynch, and M.B. Tsang, Phys. Lett. B **189**, 384 (1987).

[10] V. de la Mota, F. Sebille, M. Farine, B. Remaud, and P. Schuck, Phys. Rev. C **46**, 677 (1992).

[11] D. Krofcheck, W. Bauer, G.M. Crawley, C. Djalali, S. Howden, C.A. Ogilvie, A. Vander Molen, G.D. Westfall, and W.K. Wilson, Phys. Rev. Lett. **63**, 2028 (1989).

[12] C.A. Ogilvie, D.A. Cebra, J. Clayton, P. Danielewicz, S. Howden, J. Karn, A. Nadasen, A. Vander Molen, G.D. Westfall, W.K. Wilson, and J.S. Winfield, Phys. Rev. C **40**, 2592 (1989).

[13] J.P. Sullivan, J. Péter, D. Cussol, G. Bizard, R. Brou, M. Louvel, J.P. Patry, R. Régimbart, J.C. Steckmeyer, B. Tamain, E. Crema, H. Doubre, K. Hagel, G.M. Jin, A. Péghaire, F. Saint-Laurent, Y. Cassagnou, R. Legrain, C. Lebrun, E. Rosato, R. MacGarth, S.C. Jeong, S.M. Lee, Y. Nagashima, T. Nakagawa, M. Ogihara, J. Kasagi, and T. Motobayashi, Phys. Lett. B **249**, 8 (1990).

[14] W.M. Zhang, R. Madey, M. Elaasar, J. Schambach, D. Keane, B.D. Anderson, A.R. Baldwin, J. Cogar, J.W. Watson, G.D. Westfall, G. Krebs, and H. Wieman, Phys. Rev. C **42**, R491 (1990).

[15] D. Krofcheck, D.A. Cebra, M. Cronqvist, R. Lacey, T. Li, C.A. Ogilvie, A. Vander Molen, K. Tyson, G.D. Westfall, W.K. Wilson, and J.S. Winfield, Phys. Rev. C **43**, 350 (1991).

[16] J. Péter, Nucl. Phys. **A545**, 173c (1992).

[17] W.Q. Shen, J. Péter, G. Bizard, R. Brou, D. Cussol, M. Louvel, J.P. Patry, R. Régimbart, J.C. Steckmeyer, J.P. Sullivan, B. Tamain, E. Crema, H. Doubre, K. Hagel, G.M. Jin, A. Péghaire, F. Saint-Laurent, Y. Cassagnou, R. Legrain, C. Lebrun, E.

Rosato, R. MacGarth, S.C. Jeong, S.M. Lee, Y. Nagashima, T. Nakagawa, M. Ogihara, J. Kasagi, and T. Motobayashi, Nucl. Phys. **A551**, 333 (1993).

[18] J. Lauret, R.A. Lacey, A. Elmaani, A. Tsepetis, A. Moores, G.D. Westfall, D. Craig, E. Gualtieri, S. Hannuschke, T. Li, W.J. Llope, R. Pak, N. Stone, A. Vander Molen, J. Yee, A. Nadasen, R.S. Tickle, and E. Norbeck, Phys. Lett. B **339**, 22 (1994).

[19] A. Buta, J.C. Angélique, G. Auger, G. Bizard, R. Brou, C. Cabot, Y. Cassagnou, E. Crema, D. Cussol, Y. El Masri, Ph. Eudes, M. Gonin, K. Hagel, Z.Y. He, A. Kerambrun, C. Lebrun, R. Legrain, J.P. Patry, A. Péghaire, J. Péter, R. Popescu, R. Régimbart, E. Rosato, F. Saint-Laurent, J.C. Steckmeyer, B. Tamain, E. Vient, and R. Wada, Nucl. Phys. **A584**, 397 (1995).

[20] S. Soff, S.A. Bass, Ch. Hartnack, H. Stöcker, and W. Greiner, Phys. Rev. C **51**, 3320 (1995).

[21] R. Pak, W.J. Llope, D. Craig, E.E. Gualtieri, S.A. Hannuschke, R.A. Lacey, J. Lauret, A.C. Mignerey, D.E. Russ, N.T.B. Stone, A.M. Vander Molen, G.D. Westfall, and J. Yee, Phys. Rev. C **53**, R1469 (1996).

[22] G.D. Westfall, J.E. Yurkon, J. Van der Plicht, Z.M. Koenig, B.V. Jacak, R. Fox, G.M. Crawley, M.R. Maier, B.E. Hasselquist, R.S. Tickle, and D. Horn, Nucl. Instr. and Methods **A238**, 347 (1985).

[23] C. Cavata, M. Demoulins, J. Gosset, M.-C. Lemaire, D. L'Hôte, J. Poitou, and O. Valette, Phys. Rev. C **42**, 1760 (1990).

[24] L. Phair, D.R. Bowman, C.K. Gelbke, W.G. Gong, Y.D. Kim, M.A. Lisa, W.G. Lynch, G.F. Peaslee, R.T. de Souza, M.B. Tsang, and F. Zhu, Nucl. Phys. **A548**, 489 (1992).

[25] W.J. Llope, J.A. Conrad, C.M. Mader, G. Peilert, W. Bauer, D. Craig, E. Gualtieri, S. Hannuschke, R.A. Lacey, J. Lauret, T. Li, A. Nadasen, E. Norbeck, R. Pak, N.T.B. Stone, A.M. Vander Molen, G.D. Westfall, J. Yee, and S.J. Yennello, Phys. Rev. C **51**, 1325 (1995).

[26] W.K. Wilson, R. Lacey, C.A. Ogilvie, and G.D. Westfall, Phys. Rev. C **45**, 738 (1992).

[27] P. Danielewicz and G. Odyniec, Phys. Lett. **157B**, 146 (1985).

[28] C. Gale, G. Bertsch, and S. Das Gupta, Phys. Rev. C **35**, 1666 (1987).

[29] J. Aichelin, A. Rosenhauer, G. Peilert, H. Stöcker, and W. Greiner, Phys. Lett. **58** 1926 (1987).

[30] G.M. Welke, M. Prakash, T.T.S. Kuo, S. Das Gupta, and C. Gale, Phys. Rev. C **38**, 2101 (1988).

[31] G. Peilert, H. Stöcker, W. Greiner, A. Rosenhauer, A. Bohnet, and J. Aichelin, Phys. Rev. C **39**, 1402 (1989).

[32] C. Gale, G.M. Welke, M. Prakash, S.J. Lee, and S. Das Gupta, Phys. Rev. C **41**, 1545 (1990).

Figure Captions

Table 1: Reduced impact parameter bins. The values of $\hat{b}$ correspond to the upper limit of each bin.

Table 2: Measured values of the balance energies for ^{40}Ar+^{45}Sc reactions extracted for six reduced impact parameter bins. The errors listed are statistical.

Figure 1: Mean transverse momentum in the reaction plane versus the reduced c.m. rapidity for $Z = 2$ fragments from 155 MeV/nucleon ^{40}Ar+^{45}Sc collisions. The reduced impact parameter bins as listed in Table 1 are indicated in each panel. The straight lines are fits over the midrapidity region as described in the text.

Figure 2: Measured transverse flow in the reaction plane for $Z = 2$ fragments as a function of reduced impact parameter bins for ^{40}Ar+^{45}Sc reactions at six incident beam energies. The lines are included only to guide the eye.

Figure 3: Mean transverse momentum in the reaction plane versus the reduced c.m. rapidity for $Z = 2$ fragments in semi-central ^{40}Ar+^{45}Sc reactions (BIN3 as given in Table 1). The incident beam energy per nucleon is indicated in each panel. The straight lines are fits over the midrapidity region as described in the text.

Figure 4: Excitation functions of the measured transverse flow in the reaction plane

for $Z = 2$ fragments at six reduced impact parameter bins for ^{40}Ar+^{45}Sc reactions. The corresponding values of $\hat{b}$ are given in Table 1. The curves are included only to guide the eye.

Figure 5: Excitation functions of the measured transverse flow in the reaction plane for three fragment types at a reduced impact parameter bin of $\hat{b} = 0.39$ for ^{40}Ar+^{45}Sc reactions. The curves are included only to guide the eye.

Figure 6: Measured balance energies for ^{40}Ar+^{45}Sc reactions at six reduced impact parameter bins compared with the predictions of QMD model [20] calculations with and without momentum dependence in the mean field for ^{40}Ca+^{40}Ca reactions. The experimental values of $E_{bal}(b)$ are plotted at the upper limit of each $\hat{b}$ bin. The curves are included only to guide the eye.

Bin No.	Cut on $\hat{E}_t$	Geometric $\hat{b}$	Corrected $\hat{b}$
BIN1	top 10%	0.32	0.28
BIN2	10% - 20%	0.45	0.39
BIN3	20% - 30%	0.55	0.48
BIN4	30% - 40%	0.63	0.56
BIN5	40% - 50%	0.71	0.62
BIN6	50% - 75%	0.87	0.76
BIN7	bottom 25%	1.00	0.88

Table 1:

Corrected $\hat{b}$	E_{bal} (MeV/nucleon)
0.28	85±6
0.39	96±3
0.48	104±3
0.56	112±4
0.62	116±5
0.76	128±3

Table 2:

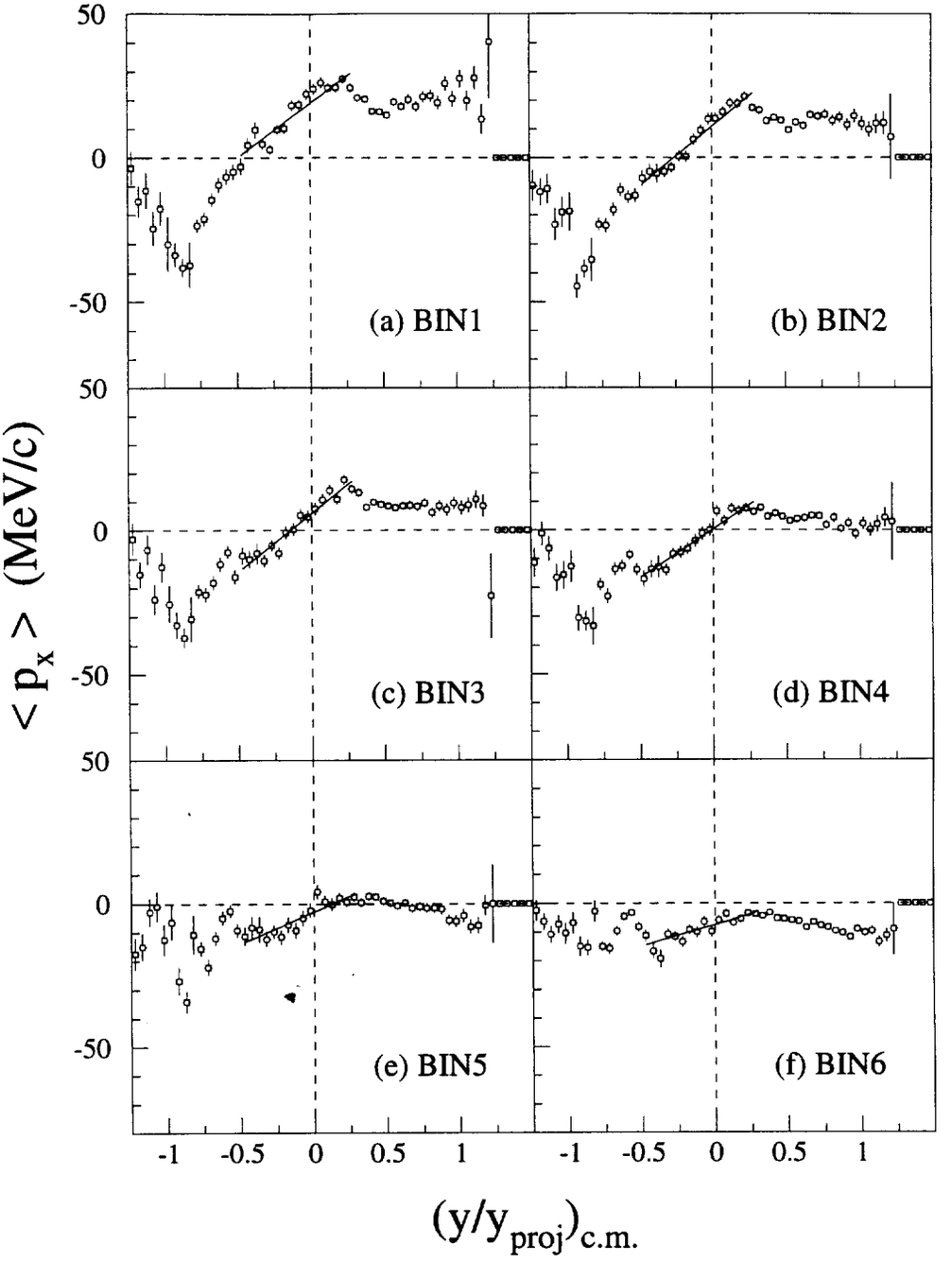
50
0
-50
(a) BIN1
(b) BIN2
(c) BIN3
(d) BIN4
(e) BIN5
(f) BIN6
-1
-0.5
0
0.5
1
< p_x > (MeV/c)
$(y/y_{proj})_{c.m.}$

Figure 1:

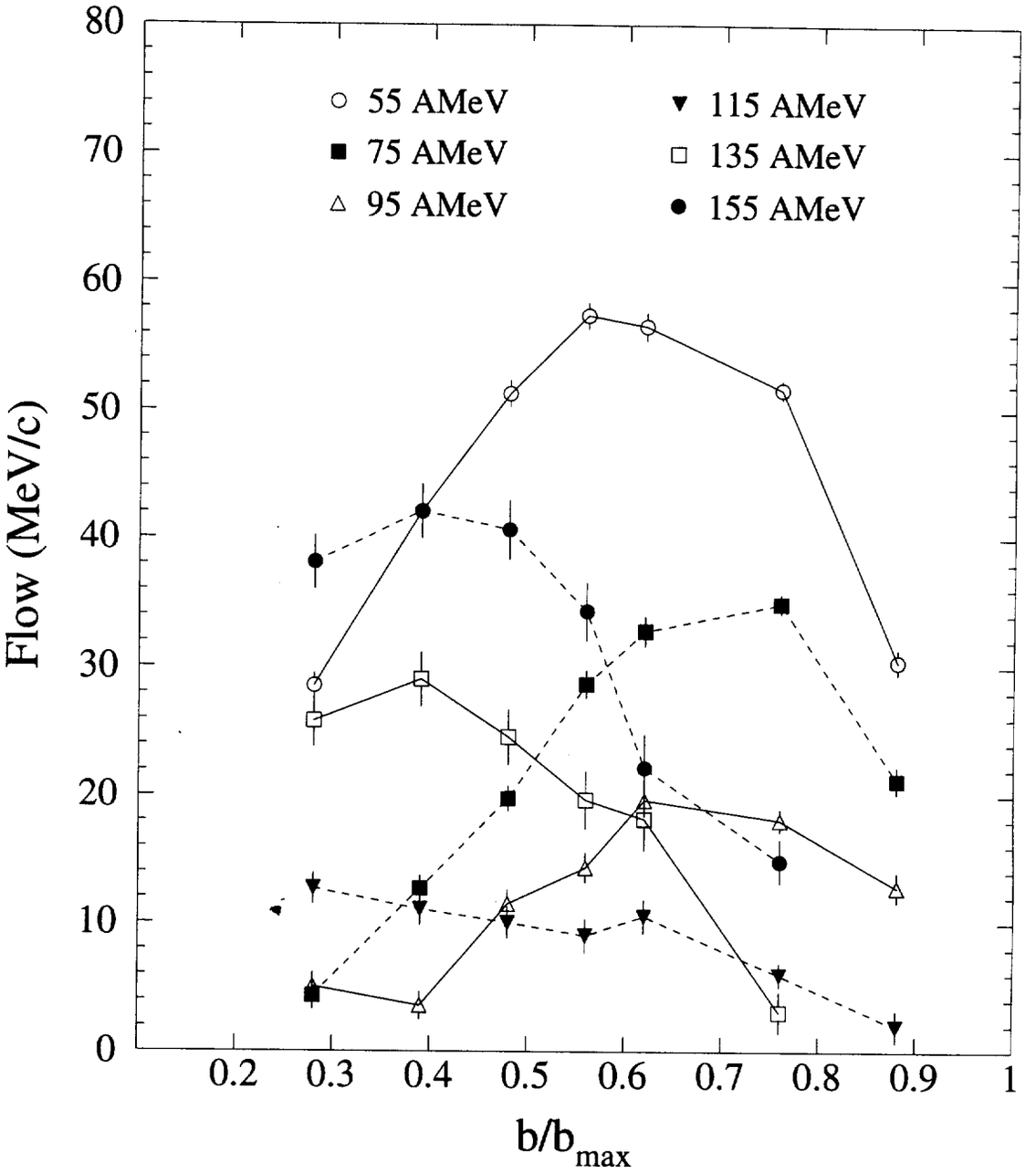
55 AMeV
75 AMeV
95 AMeV
115 AMeV
135 AMeV
155 AMeV
Flow (MeV/c)
b/b_max
0
10
20
30
40
50
60
70
80
0.2
0.3
0.4
0.5
0.6
0.7
0.8
0.9
1

Figure 2:

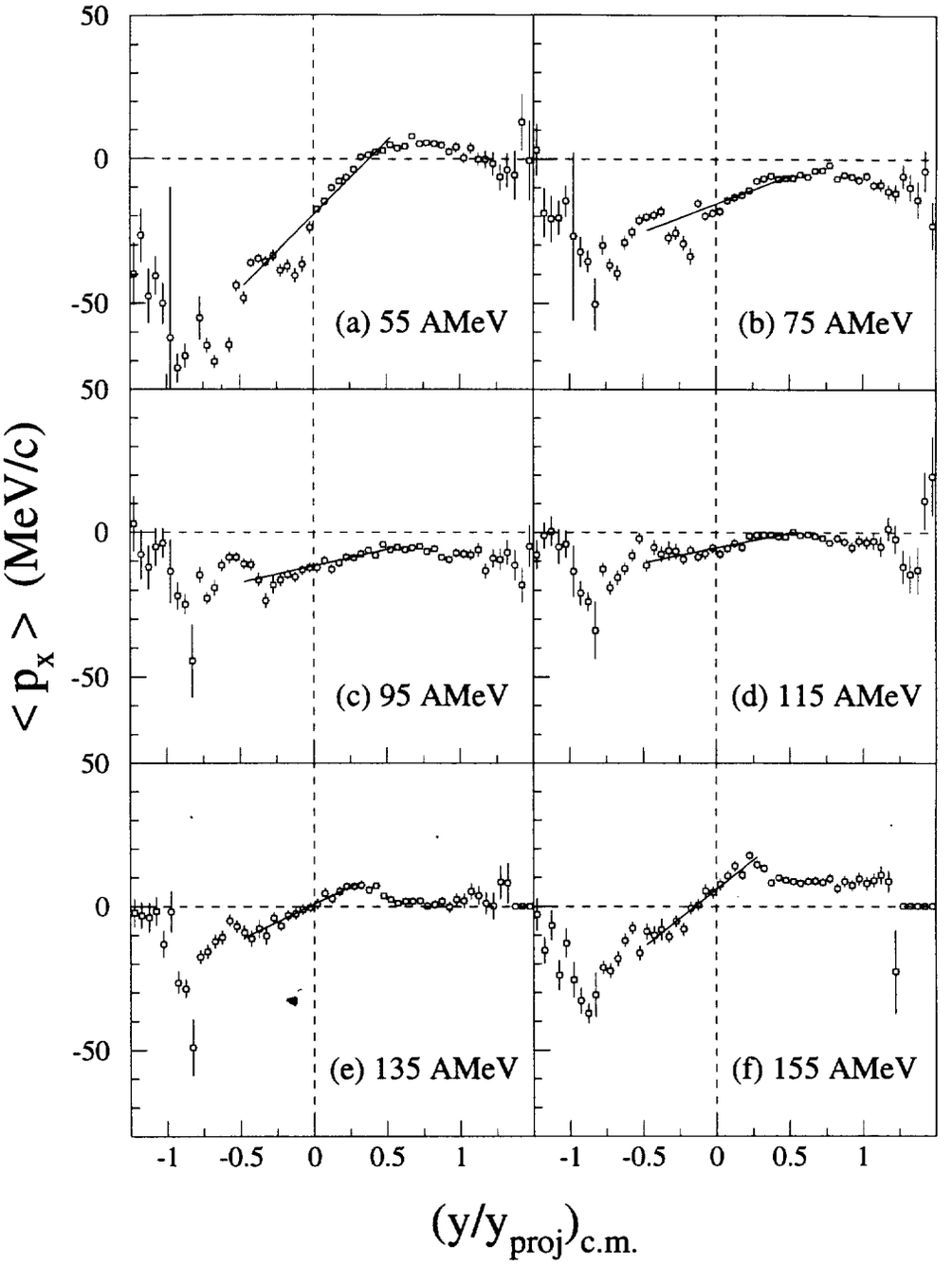
50
0
-50
(a) 55 AMeV
(b) 75 AMeV
(c) 95 AMeV
(d) 115 AMeV
(e) 135 AMeV
(f) 155 AMeV
< p_x > (MeV/c)
-1
-0.5
0
0.5
1
$(y/y_{proj})_{c.m.}$

Figure 3:

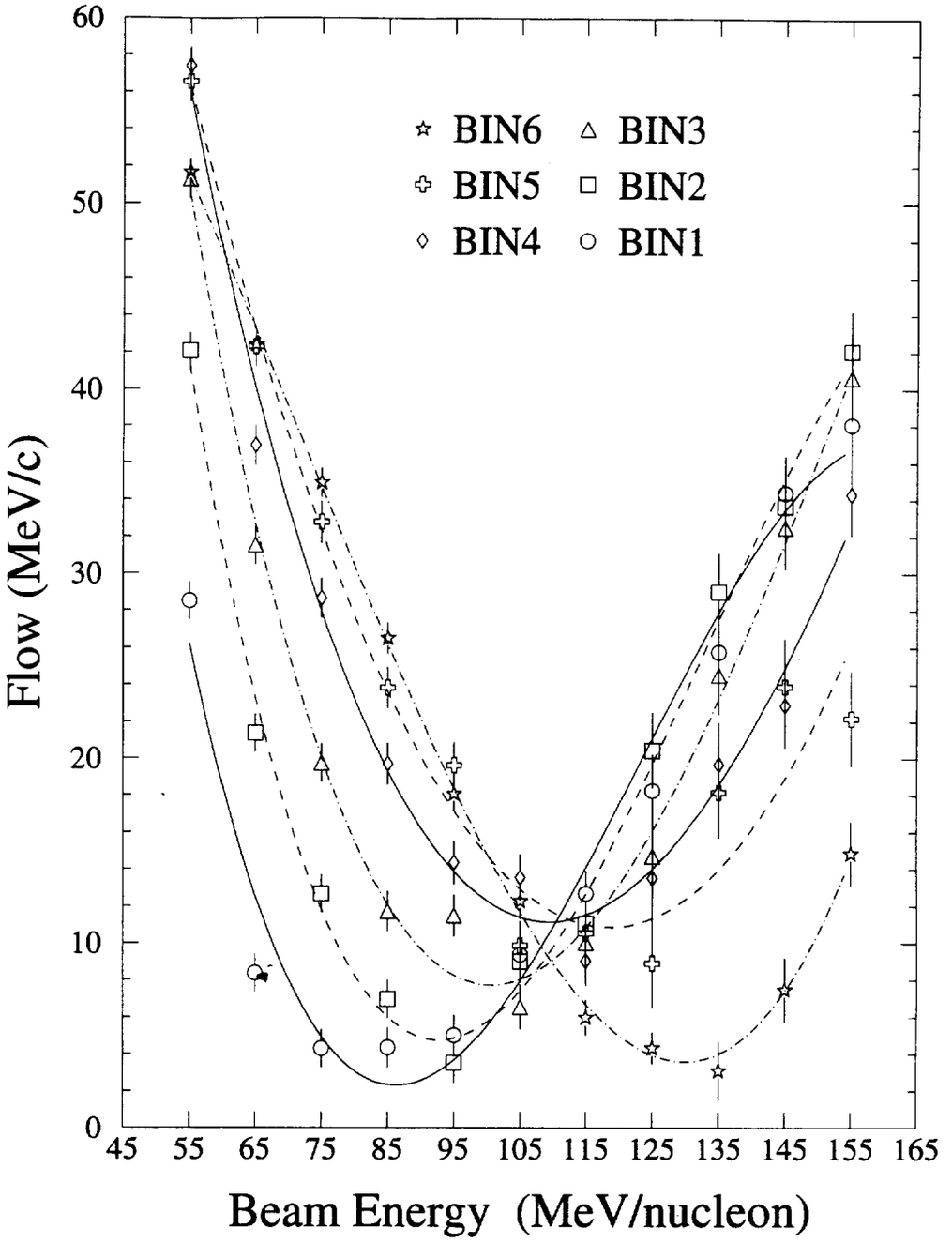
BIN6
BIN5
BIN4
BIN3
BIN2
BIN1
Flow (MeV/c)
Beam Energy (MeV/nucleon)
0
10
20
30
40
50
60
45
55
65
75
85
95
105
115
125
135
145
155
165

Figure 4:

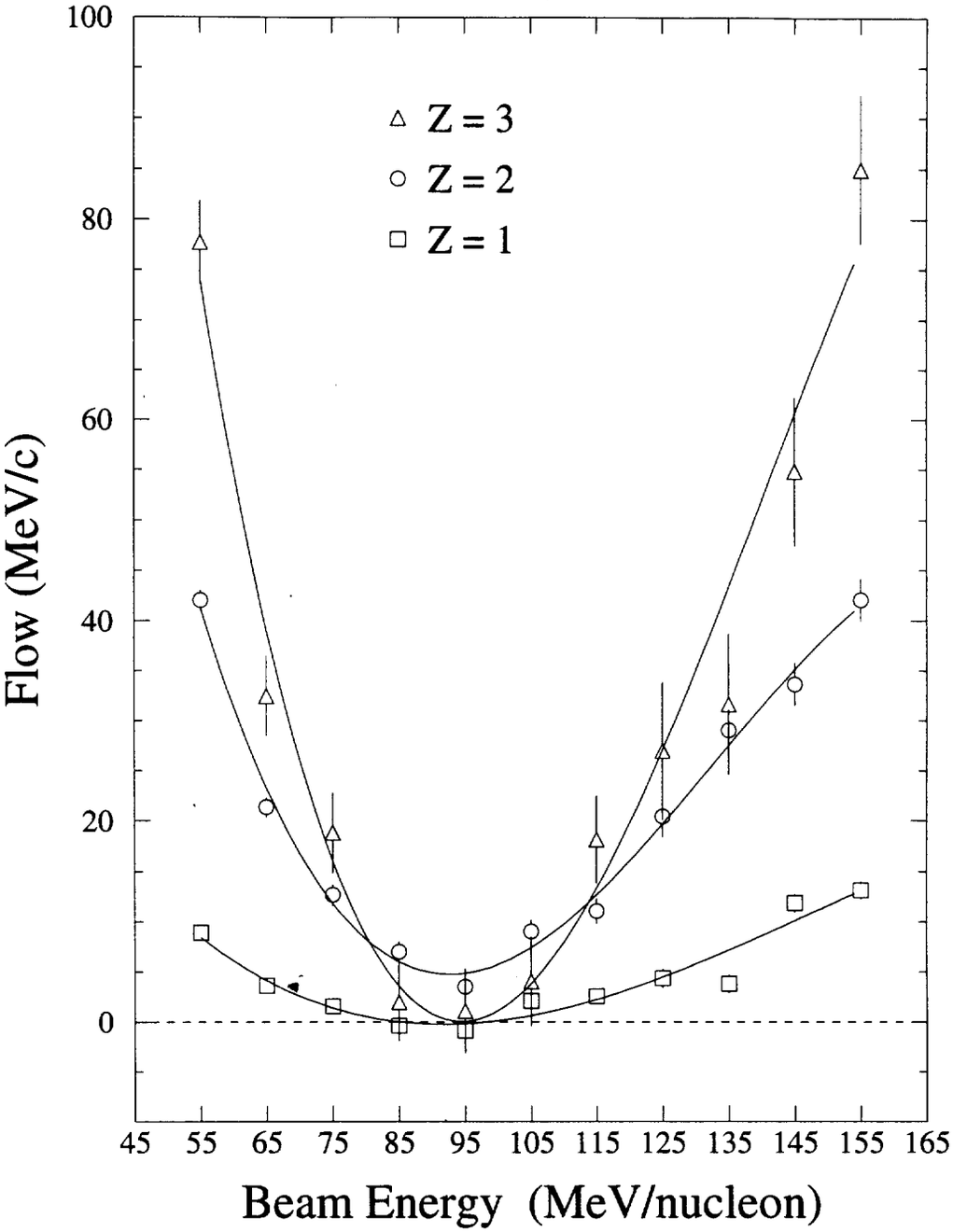
Z = 3
Z = 2
Z = 1
Flow (MeV/c)
Beam Energy (MeV/nucleon)
100
80
60
40
20
0
45
55
65
75
85
95
105
115
125
135
145
155
165

Figure 5:

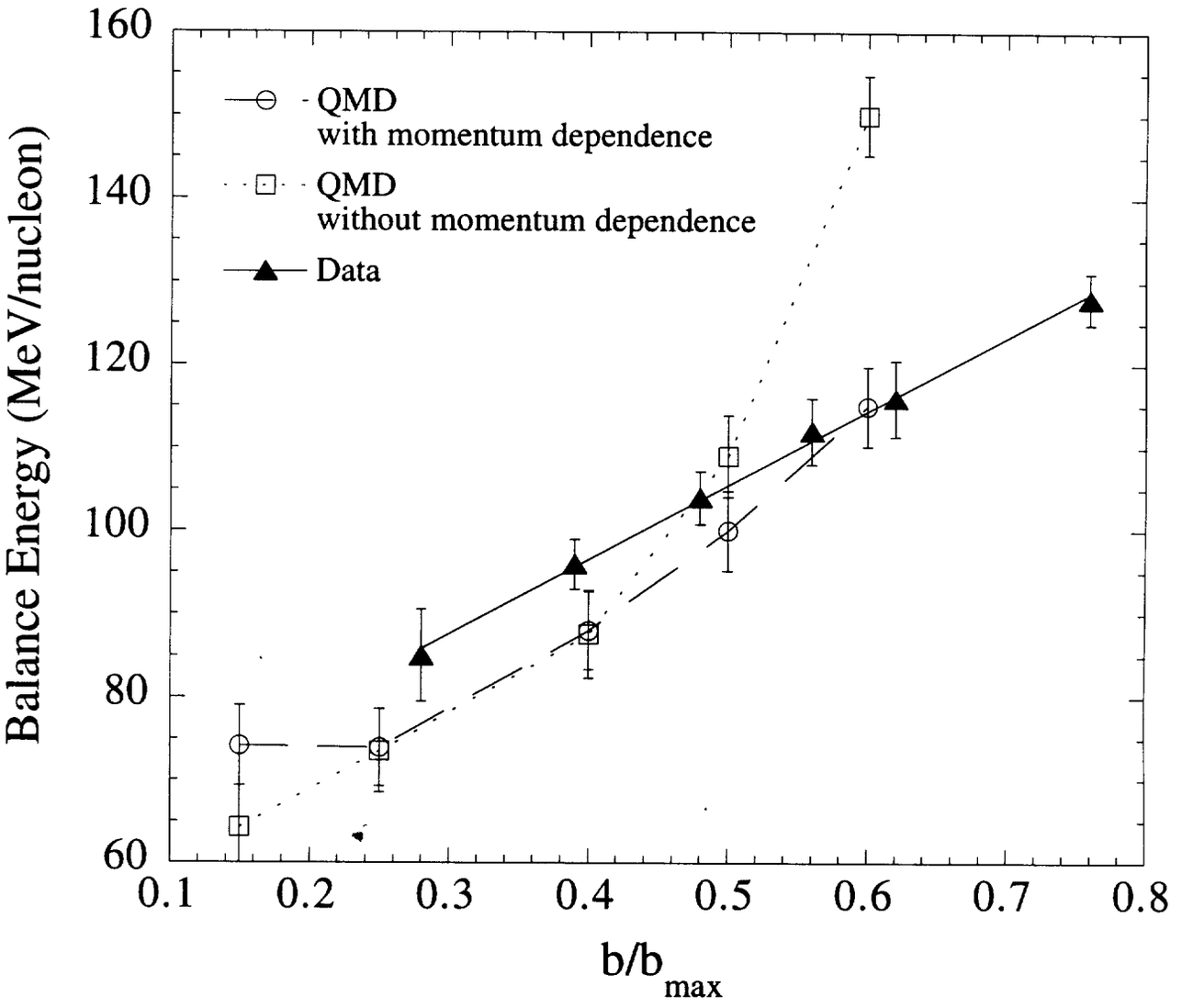
160
140
120
100
80
60
0.1
0.2
0.3
0.4
0.5
0.6
0.7
0.8
Balance Energy (MeV/nucleon)
b/b max
QMD
with momentum dependence
QMD
without momentum dependence
Data

Figure 6: